CSIRO PUBLISHING

Australian Journal of Physics

Volume 53, 2000

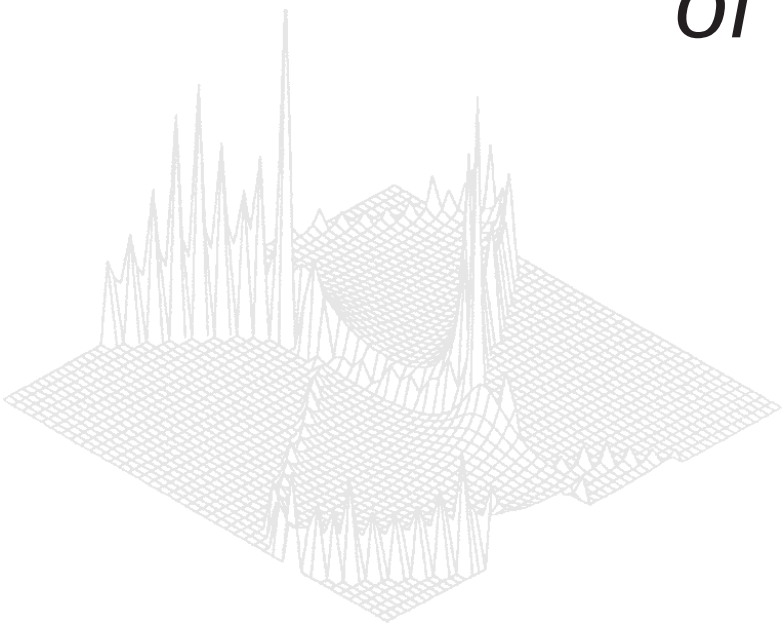

A journal for the publication of
original research in all branches of physics

www.publish.csiro.au/journals/ajp

All enquiries and manuscripts should be directed to
Australian Journal of Physics
CSIRO PUBLISHING
PO Box 1139 (150 Oxford St)
Collingwood Telephone: 61 3 9662 7626
Vic. 3066 Facsimile: 61 3 9662 7611
Australia Email: ajp@publish.csiro.au

Published by **CSIRO** PUBLISHING
for CSIRO and
the Australian Academy of Science

Aust. J. Phys., 2000, **53**, 665–688

Ro–vibrational Transition Energies and Absorption Intensities of the $^1A_1$ States of H_2O, He_2O^{2+} and He_2S^{2+}

Sudarko, J. M. Hughes and E. I. von Nagy-Felsobuki[A]

School of Biological and Chemical Sciences, University of Newcastle,
Callaghan, NSW 2308, Australia.
[A] Corresponding author: chvo@cc.newcastle.edu.au

Abstract

Variational ro–vibrational wave functions are calculated using an Eckart–Watson Hamiltonian, which has embedded an ab initio potential energy function. These wave functions, together with an ab initio dipole moment function, are employed to predict transition energies and absorption intensities. The radiative transition probability integrals are determined using a novel adaptation of the Harris–Engerholm–Gwinn integration scheme. The method and solution algorithm yields results in excellent agreement with previously determined experimental and theoretical electric dipole allowed transitions for the $^1A_1$ ground state of H_2O. The method has also been applied to the $^1A_1$ states of the helide analogs of water, namely He_2O^{2+} and He_2S^{2+}, in order to predict their ro–vibrational transition energies and absorption intensities, thereby facilitating their possible interstellar detection.

1. Introduction

Due to the inert nature of helium, the chemistry of interstellar gas clouds has largely centred on hydrogen (see e.g. Green 1981). There has been a resurgence of interest in helide chemistry due to theoretical investigations which predict that helide cations are much more strongly bound than their neutral counterparts (see e.g. Koch and Frenking 1986; Wong *et al.* 1987; Frenking and Cremer 1990). Impetus has also come from experiment, where mass spectral investigations have identified ions of the form $HeNg^+$ and NgX^{n+} (where Ng is Ne, Ar, Kr or Xe; X is C, N or O; and n = 1, 2) (Munson *et al.* 1963). With the exception of $HeXe^+$, only the former cations have been spectroscopically observed (Dabrowski and Herzberg 1978). More recently, a high-resolution vibration–rotation spectrum of HeH^+ has also been reported (Bernath and Amano 1982). For larger helide ions, only metastable species such as N_2^+–$(He)_n$ (n = 1–3) (Bieske *et al.* 1992) and He_n–HN_2^+ (n = 1, 2) (Meuwly *et al.* 1996) have been spectroscopically characterised.

The ro–vibrational spectrum for the $^1A_1$ state of water and its helide analogs (such as He_2O^{2+} and He_2S^{2+}) is of considerable interest in a variety of fields ranging from astronomy and astrophysics to studies involving the atmosphere of planets (see e.g. Dudley and Williams 1984; Jørgensen 1994). In the case of water, there are considerable experimental data culminating in the HITRAN 92 (Rothman *et al.* 1992) and HITRAN 96 (Rothman *et al.* 1998) data bases. However, there are no experimental ro–vibrational transition energies and absorption intensities for He_2O^{2+} and He_2S^{2+} in the literature.

There are numerous ab initio calculations of the ground state of water, with the extensive calculations of Partridge and Schwenke (PS) (1997) yielding a comprehensive spectroscopic characterisation of the molecule. However, for the helide analogs there are only a few theoretical calculations. Using the MP2_AE/6-31G(d, p) level of theory, Koch

 10.1071/PH00027 0004-9506/00/050665$05.00

and Frenking (1986) predicted that the $^1A_1$ state of He_2O^{2+} is metastable, with equilibrium bond length and bond angle of 1.148 Å and 92.2° respectively. Hughes and von Nagy-Felsobuki (1997), using the CCSD(T)_AE/cc-pCVTZ model, yielded structural parameters of 1.168 Å and 92.6° respectively. They have also calculated ro–vibrational eigenenergies of the low-lying ro–vibrational states. The only structural parameters for the $^1A_1$ state of He_2S^{2+} were calculated by Hughes and von Nagy-Felsobuki (1999) using the CCSD(T)_FC/cc-pVTZ level of theory (which yielded parameters of 1.665 Å and 77.0° respectively). There are no calculated ro–vibrational transition energies and absorption intensities of He_2O^{2+} and He_2S^{2+}.

With the advent of supercomputers, significant progress has been made in developing algorithms for computing ab initio ro–vibrational energy levels and intensities for triatomic molecules. In the case of the electronic wave function, accurate potential energy surfaces (PES) can be constructed from discrete electronic calculations employing extensive particle basis sets within theories that incorporate high levels of electron correlation (see e.g. Meyer *et al.* 1986). Although ro–vibrational calculations are still not commonplace, they are usually obtained utilising ro–vibrational Hamiltonians (cast in differing coordinate systems) and using either analytical or numerical vibrational basis sets (see e.g. Searles and von Nagy-Felsobuki 1991, 1993). While ro–vibrational transition energies for different algorithms have been shown to converge for a given PES (see e.g. Searles and von Nagy-Felsobuki 1989; Wang and von Nagy-Felsobuki 1992, 1995), calculating ro–vibrational absorption intensities requires the construction of an additional property of a molecule; namely, its dipole moment surface (DMS). Hence, the accuracy of ab initio absorption intensities is a severe test of the accuracy of the PES and DMS as well as of the robustness of the solution algorithm (e.g. convergence of the ro–vibrational wave functions and the evaluation of energy and transition probability integrals).

As an extension of our previous work in developing an integrated suite of programs to calculate spectroscopic properties of triatomic molecules (see e.g. Searles and von Nagy-Felsobuki 1988, 1991, 1992, 1993; Wang and von Nagy-Felsobuki 1992, 1995) we wish to present a general approach for the calculation of absorption intensities. We shall therefore detail several 'new' property surfaces, namely, an ab initio PES for the $^1A_1$ state of He_2S^{2+} and the DMS for He_2O^{2+} and He_2S^{2+}. We shall benchmark the experimental (see e.g. Rothman *et al.* 1992, 1998) and theoretical (see e.g. PS 1997) ro–vibrational transition energies and absorption intensities of H_2O with those calculated using our solution algorithm (which incorporates a novel integration scheme for the calculation of radiative transition probabilities). We shall also detail the predicted transition energies, absorption intensities of the $^1A_1$ states of He_2O^{2+} and He_2S^{2+} (which are isovalent with H_2O), thereby assisting in their possible spectroscopic detection.

2. Discrete Ab Initio Property Surfaces

Generally, the basis sets employed were the correlation consistent polarised valence X zeta (cc-pVXZ) basis sets of Woon and Dunning (1994, 1995). Here X represents the degree of expansion.

For H_2O, a 771 point PES and DMS is available from the work of PS (1997). These discrete surfaces were calculated using the aug-cc-pV5Z (quintal zeta) basis set, within an internal contraction multi-reference configuration interaction (denoted ICMRCI) model coupled with a multi-reference Davidson correction (+Q). The ICMRCI+Q/aug-cc-pV5Z discrete energies and dipole moments surfaces are available from E-PAPS (1997).

For He_2O^{2+}, a discrete 68 point PES is also available from the literature (Hughes and von Nagy-Felsobuki 1997). It was calculated using an all-electron couple cluster method involving single and double excitations with a perturbation estimation of the triple excitations [denoted CCSD(T)_AE] and a cc-pCVTZ basis set. Oliphant and Bartlett (1994) showed that using the same level of theory, the average errors for H_2O with respect to bond lengths, bond angles, frequencies and atomisation energies were in the range 0.0 Å, 0.3°, ≈13–21 cm^{-1} and 41.0 kJ mol^{-1} respectively. It would be anticipated that the discrepancies for these properties in the case of He_2O^{2+} would be of a similar order of magnitude.

There is no discrete PES available for He_2S^{2+}. Consequently, a discrete PES was constructed using standard ab initio calculations employing the GAUSSIAN 94 suite of programs (Frisch *et al.* 1995). The level of theory used was the frozen-core CCSD(T)_FC/cc-pVQZ (quadrupole zeta) model. It would be anticipated that for a helide ion containing a second-row atom and using the frozen-core approximation, larger discrepancies should occur in bond lengths, bond angles, frequencies and atomisation energies than for either H_2O or He_2O^{2+}.

For the construction of the discrete PES, ab initio electronic points were chosen to be nearly coincident to the quadrature points required by Harris, Engerholm and Gwinn (HEG) (1965). This ensures that the error of the fit associated with the potential energy function is minimised. For He_2O^{2+} and He_2S^{2+} the HEG scheme uses 8000 quadrature points, which would render the electronic problem intractable. To cull the possible calculations, an adaptive strategy was employed, the details of which have been described elsewhere (Searles and von Nagy-Felsobuki 1993; Hughes and von Nagy-Felsobuki 1997). Table 1 lists the 98 points on the potential energy hypersurface for He_2S^{2+}. The instantaneous displacements from equilibrium bond length are all less than $2.0r_e$ and so the potential energy surface is concentrated near the potential well in order to ensure a highly accurate surface. Using the CCSD(T)_FC/cc-pVQZ level of theory, the optimised structure for the $^1A_1$ ground state of He_2S^{2+} is calculated to be of C_{2v} symmetry, with bond length and bond angle of 1.6504 Å and 76.6° respectively, yielding a minimum energy of –402.2374016 E_h.

There are no discrete DMS available for He_2O^{2+} and He_2S^{2+}. Dipole moments using the GAUSSIAN suite of programs are not available at the CCSD(T) level of theory. The level of theory used in the construction of the DMS for He_2O^{2+} and He_2S^{2+} was the QCISD_AE/aug-cc-pCVTZ and QCISD_FC/aug-cc-pVTZ respectively. All calculations were performed in the centre-of-mass coordinate system (and not in the centre-of-charge system, the default option in GAUSSIAN).

Green (1974) concluded that for a diatomic molecule with a single sigma bond, the error in the dipole moment at the Hartree–Fock (HF) limit is of the order of ~0.1 to 0.2 D. Furthermore, he noted that a similar order of accuracy could be achieved provided the basis set was at least double zeta in size and augmented with polarisation functions. Oliphant and Bartlett (1994) showed that the average error for polyatomic molecules, at the HF level using large size basis sets, was of a similar order (i.e. 0.29 D). Hence, we would anticipate that for He_2O^{2+} and He_2S^{2+} discrepancies no larger than 0.3 D should occur for the discrete ab initio DMS.

For the construction of the discrete DMS, ab initio points were also chosen to be nearly coincident to the quadrature points as required by the HEG scheme. A similar adaptive strategy for the construction of the discrete PES was chosen for the construction of the discrete DMS. Table 2 lists the 58 and 70 points on the dipole moment hypersurface for

Table 1. Discrete potential energy surface of the $^1A_1$ ground state of He_2S^{2+}

[using the CCSD(T)_FC/cc-pVQZ level of theory]

All bond lengths are in atomic units and all energies are in Hartrees

r_{He-S}	r'_{He-S}	r_{He-He}	E/E_h	r_{He-S}	r'_{He-S}	r_{He-He}	E/E_h
3.1188	3.1188	3.8661	-402.2374016	3.5829	2.8125	4.0017	-402.2292028
3.1974	3.1974	3.9635	-402.2370646	3.1269	3.8973	4.3881	-402.2295809
3.0402	3.0402	3.7687	-402.2370066	2.1489	3.3044	3.4788	-402.1399763
3.2760	3.2760	4.0610	-402.2361588	3.8937	2.7382	4.1921	-402.2223671
2.9617	2.9617	3.6713	-402.2356823	2.5070	4.0474	4.2082	-402.2031983
3.3153	3.3153	4.1097	-402.2355358	1.9572	3.4974	3.5545	-402.0488337
2.9224	2.9224	3.6225	-402.2345989	4.0975	3.7123	4.8483	-402.2209146
3.5118	3.5118	4.3533	-402.2312674	4.3551	2.0457	4.2951	-402.0837369
2.7259	2.7259	3.3790	-402.2234560	3.1885	3.0340	3.9780	-402.2369047
3.7083	3.7083	4.5968	-402.2259952	2.7188	3.4925	4.1238	-402.2260422
2.5294	2.5294	3.1354	-402.1977749	2.9364	3.3205	3.7659	-402.2349933
3.9048	3.9048	4.8404	-402.2205425	3.8796	2.3322	4.2330	-402.1785163
2.3329	2.3329	2.8918	-402.1464934	3.7533	2.6226	3.4162	-402.2149781
4.2978	4.2978	5.3275	-402.2106482	2.5752	3.7203	3.6844	-402.2136473
1.9399	1.9399	2.4047	-401.8679618	3.3216	2.9377	4.9770	-402.2296824
3.1112	3.1112	3.9764	-402.2372916	3.1060	3.4931	4.3941	-402.2342417
3.1284	3.1284	3.7558	-402.2372613	3.1514	3.5335	3.8438	-402.2335686
3.1056	3.1056	4.0868	-402.2369809	3.1410	2.7594	3.3581	-402.2301456
3.1398	3.1398	3.6455	-402.2368157	2.7137	3.1010	3.9081	-402.2282598
3.1034	3.1034	4.1419	-402.2367645	3.8316	2.7000	3.5108	-402.2193213
3.1461	3.1461	3.5903	-402.2364592	2.7767	4.3051	4.2241	-402.2198807
3.1850	3.1850	3.3145	-402.2329712	2.6385	2.4863	4.2400	-402.1741962
3.1001	3.1001	4.4177	-402.2352780	3.8766	2.7137	4.7341	-402.2201105
3.2351	3.2351	3.0387	-402.2255324	1.7420	2.9029	3.5414	-401.8581831
3.1088	3.1088	4.6935	-402.2335242	3.8967	3.5109	5.7067	-402.2254161
3.1296	3.1296	4.9693	-402.2319379	2.8829	4.3743	3.6944	-402.2210510
3.2958	3.2958	2.7629	-402.2119718	4.4943	4.4943	5.5711	-402.2064999
3.2060	3.2060	5.5209	-402.2301589	1.7434	1.7434	2.1611	-401.5339923
3.4468	3.4468	2.2113	-402.1500149	4.6908	4.6908	5.8147	-402.2029200
3.0418	3.1959	3.8677	-402.2370288	1.5469	1.5469	1.9175	-400.9224959
3.2730	2.9648	3.8724	-402.2358915	3.2609	3.2609	5.7967	-402.2299900
2.9263	3.3115	3.8759	-402.2350200	3.5358	3.5358	1.9355	-402.0863300
2.7339	3.5044	3.9053	-402.2271164	3.3261	3.3261	6.0725	-402.2300932

Table 1 (*Continued*)

$r_{He\text{-}S}$	$r'_{He\text{-}S}$	$r_{He\text{-}He}$	E/E_h	$r_{He\text{-}S}$	$r'_{He\text{-}S}$	$r_{He\text{-}He}$	E/E_h
3.6973	2.5418	3.9537	-402.2112066	3.6331	3.6331	1.6597	-401.9858057
3.8903	2.3499	4.0204	-402.1823548	1.7768	4.4697	4.3213	-401.8883601
4.2765	1.9673	4.2054	-402.0430177	1.5871	4.6630	4.4514	-401.6178880
2.3499	3.8903	4.0204	-402.1823548	4.4697	1.7768	4.3213	-401.8883601
1.9673	4.2765	4.2054	-402.0430177	4.6630	1.5871	4.4514	-401.6178880
3.2069	3.2069	3.8532	-402.2368643	4.5489	4.5489	7.5017	-402.2054937
2.9442	2.9442	4.2229	-402.2318501	2.0875	2.0875	4.0917	-401.8556920
3.2626	3.2626	4.2816	-402.2361111	1.8507	4.7591	6.2024	-401.9524722
3.4957	3.4957	5.1807	-402.2305321	4.8425	2.5747	2.5460	-402.1850000
2.7113	2.7113	3.6548	-402.2201124	3.1545	6.2341	6.2192	-402.2179979
3.9141	3.9141	4.7301	-402.2202827	3.2270	5.8867	7.7462	-402.2180300
3.6790	3.6790	3.2501	-402.2183014	4.3153	5.7514	4.0377	-402.2004418
2.4067	2.4067	2.3402	-402.1386090	3.4842	4.6006	7.0952	-402.2198785
2.9632	3.1173	3.7703	-402.2365248	5.0559	3.8954	6.7254	-402.2104434
3.3924	3.2383	4.1112	-402.2353618	1.4659	2.1990	3.3106	-401.2048147
3.3193	3.7045	4.3620	-402.2309346	5.6900	4.5414	8.2739	-402.1991753

He_2O^{2+} and He_2S^{2+} respectively. For the optimised equilibrium structures, the dipole moment was calculated to be 1.7026 D and 0.2373 D respectively.

3. Analytical Representations of the Discrete Property Surfaces

For H_2O, the potential function fitted to the discrete ICMRCI+Q/aug-cc-pV5Z PES has been detailed by PS (1997). It is a many-body potential of the Murrell type involving one-, two- and three-body terms. The fitting parameters were determined either from an unequal weighted least squares fit or pre-determined to reproduce preliminary estimates of the molecular shape. A subroutine to evaluate this fit is available from E-PAPS (1997).

For He_2O^{2+}, a multi-dimensional least squares fit of the discrete CCSD(T)_AE/cc-pCVTZ PES using singular value decomposition (SVD) analysis has been reported elsewhere (Hughes and von Nagy-Felsobuki 1997). This approach employed Padé approximates, which are rational functions, with the numerator and denominator being power series expansions of order m and n respectively [labelled as $P(m,n)$]. The most 'appropriate' potential function was the $P(4,5)$ analytical representation, which utilised an Ogilvie expansion variable (Hughes and von Nagy-Felsobuki 1997). Singular values σ_{50} and σ_{52-55} were set to zero in order to ensure that no oscillatory behaviour or singularities occurred in the integration region.

The approach outlined by Hughes and von Nagy-Felsobuki (1997) was used to fit the analytical representation of the discrete CCSD(T)_FC/cc-pVQZ PES of He_2S^{2+}. A number of analytical representations were investigated, using a variety of expansion variables (see e.g. Searles and von Nagy-Felsobuki 1993) for power series up to order 7, and Padé approximates up to order 6 (in both the numerator and denominator series). The 'best'

Table 2. Discrete dipole moment surface for He_2O^{2+} and He_2S^{2+}

Dipole moments and bond lengths are in atomic units and bond angles are in degrees

He_2O^{2+}					He_2S^{2+}				
$r_{He\text{-}O}$	$r'_{He\text{-}O}$	α	μ_y	μ_x	$r_{He\text{-}S}$	$r'_{He\text{-}S}$	α	μ_y	μ_x
2.2076	2.2076	92.5682	0.6698	0.0000	3.1188	3.1188	76.6029	0.0934	0.0000
2.2915	2.2915	92.5682	0.6234	0.0000	3.1974	3.1974	76.6029	0.0266	0.0000
2.1237	2.1237	92.5682	0.7197	0.0000	3.0402	3.0402	76.6029	0.1597	0.0000
2.4174	2.4174	92.5682	0.5609	0.0000	3.3153	3.3153	76.6029	-0.0739	0.0000
1.9978	1.9978	92.5682	0.7987	0.0000	2.9224	2.9224	76.6029	0.2576	0.0000
2.6272	2.6272	92.5682	0.4778	0.0000	3.5118	3.5118	76.6029	-0.2407	0.0000
1.7880	1.7880	92.5682	0.9244	0.0000	2.7259	2.7259	76.6029	0.4135	0.0000
2.8369	2.8369	92.5682	0.4245	0.0000	3.7083	3.7083	76.6029	-0.4038	0.0000
1.5782	1.5782	92.5682	1.0031	0.0000	2.5294	2.5294	76.6029	0.5525	0.0000
3.0467	3.0467	92.5682	0.4119	0.0000	3.9048	3.9048	76.6029	-0.5608	0.0000
1.3684	1.3684	92.5682	1.0097	0.0000	2.3329	2.3329	76.6029	0.6625	0.0000
3.4663	3.4663	92.5682	0.6438	0.0000	4.2978	4.2978	76.6029	-0.8496	0.0000
0.9489	0.9489	92.5682	0.8732	0.0000	1.9399	1.9399	76.6029	0.7512	0.0000
2.1922	2.1922	97.0866	0.6649	0.0000	3.1112	3.1112	79.4410	0.1043	0.0000
2.2264	2.2264	88.1193	0.6689	0.0000	3.1284	3.1284	73.7803	0.0793	0.0000
2.1755	2.1755	103.9665	0.6464	0.0000	3.1034	3.1034	83.7199	0.1152	0.0000
2.2607	2.2607	81.6009	0.6569	0.0000	3.1461	3.1461	69.5826	0.0522	0.0000
2.3336	2.3336	71.2273	0.6118	0.0000	3.1850	3.1850	62.7084	-0.0095	0.0000
2.1655	2.1655	115.5871	0.5871	0.0000	3.1001	3.1001	90.8801	0.1194	0.0000
2.4243	2.4243	61.5552	0.5482	0.0000	3.2351	3.2351	56.0233	-0.0921	0.0000
2.1778	2.1778	127.1955	0.4958	0.0000	3.1088	3.1088	98.0278	0.1084	0.0000
2.2121	2.2121	138.5584	0.3812	0.0000	3.1296	3.1296	105.1081	0.0856	0.0000
2.5309	2.5309	52.6390	0.5003	0.0000	3.2958	3.2958	49.5631	-0.1944	0.0000
2.3421	2.3421	159.7765	0.1408	0.0000	3.2060	3.2060	118.8637	0.0193	0.0000
2.7846	2.7846	37.0818	0.6623	0.0000	3.4468	3.4468	37.4201	-0.4310	0.0000
2.1212	2.2941	92.5334	0.6719	-0.0402	3.0418	3.1959	76.5951	0.0935	-0.0535
1.9920	2.4240	92.3487	0.6825	-0.0984	2.9263	3.3115	76.5541	0.0940	-0.1332
1.7776	2.6410	91.6651	0.7193	-0.1781	2.7339	3.5044	76.4056	0.0956	-0.2617
2.8586	1.5647	90.4350	0.7782	0.2078	3.6973	2.5418	76.1505	0.0966	0.3812
3.0765	1.3543	88.4945	0.8679	0.1399	3.8903	2.3499	75.7761	0.0942	0.4871
1.3543	3.0765	88.4945	0.8679	-0.1399	2.3499	3.8903	75.7761	0.0942	-0.4871
3.5132	0.9468	81.0194	1.3196	-0.5423	4.2765	1.9673	74.5812	0.0602	0.6446
0.9468	3.5132	81.0194	1.3196	0.5423	1.9673	4.2765	74.5812	0.0602	-0.6446
2.3102	2.3102	88.2808	0.6232	0.0000	3.2069	3.2069	73.8494	0.0124	0.0000
2.0013	2.0013	117.5046	0.6879	0.0000	2.9442	2.9442	91.6404	0.2456	0.0000
2.3475	2.3475	101.0124	0.5653	0.0000	3.2626	3.2626	82.0173	-0.0195	0.0000
2.5814	2.5814	121.6503	0.3582	0.0000	3.4957	3.4957	95.6331	-0.1867	0.0000

Table 2 (*Continued*)

He_2O^{2+}					He_2S^{2+}				
$r_{He\text{-}O}$	$r'_{He\text{-}O}$	α	μ_y	μ_x	$r_{He\text{-}S}$	$r'_{He\text{-}S}$	α	μ_y	μ_x
1.7585	1.7585	106.6819	0.9070	0.0000	2.7113	2.7113	84.7508	0.4353	0.0000
3.0651	3.0651	89.3370	0.4187	0.0000	3.9141	3.9141	74.3470	-0.5783	0.0000
2.9288	2.9288	58.2463	0.4098	0.0000	3.6790	3.6790	52.4250	-0.5022	0.0000
1.5169	1.5169	59.4690	0.9932	0.0000	2.4067	2.4067	58.1807	0.5174	0.0000
2.0373	2.2101	92.5305	0.7217	-0.0396	2.9632	3.1173	76.5947	0.1597	-0.0524
2.5038	2.3310	92.5391	0.5627	0.0389	3.3924	3.2383	76.5960	-0.0736	0.0552
2.4115	2.8435	92.4136	0.4863	-0.0858	3.3193	3.7045	76.5644	-0.2376	-0.1379
2.7249	1.8614	91.7323	0.6729	0.1828	3.5829	2.8125	76.4154	0.0310	0.2662
2.1967	3.0604	91.9376	0.5155	-0.1651	3.1269	3.8973	76.4478	-0.2283	-0.2719
1.1471	2.4395	89.1573	0.9364	-0.0112	2.1489	3.3044	76.0041	0.3788	-0.3075
3.0682	1.7739	90.8152	0.6720	0.2359	3.8937	2.7382	76.2041	-0.0577	0.3957
1.5209	3.2441	89.1290	0.7992	-0.1986	2.5070	4.0474	75.8580	-0.0190	-0.5063
3.2630	2.8310	92.4535	0.4244	0.0207	1.9572	3.4974	75.4987	0.3435	-0.3827
3.5969	1.0279	82.1909	1.3268	-0.5076	4.0975	3.7123	76.5718	-0.5557	0.1303
2.2792	2.1052	97.0582	0.6670	0.0417	4.3551	2.0457	74.6938	0.0210	0.6657
1.7434	2.6182	101.1006	0.7027	-0.1873	3.1885	3.0340	79.4349	0.1044	0.0551
2.0128	2.4411	87.8636	0.6812	-0.0959	2.7188	3.4925	82.1809	0.1115	-0.2782
3.0569	1.3092	99.1001	0.8570	0.1049	2.9364	3.3205	73.7213	0.0803	-0.1295
2.9570	1.7380	67.8590	0.6799	0.2309	3.8796	2.3322	81.8281	0.1015	0.5207
1.6389	2.8998	78.7035	0.7536	-0.2172	3.7533	2.6226	61.8281	0.0126	0.3292
2.4281	1.9970	138.7876	0.3848	0.1769	2.5752	3.7203	68.9011	0.0643	-0.3533
2.1655	2.6035	102.8626	0.5507	-0.1047	3.3216	2.9377	105.1682	0.0826	0.1792
2.2590	2.6818	82.2849	0.5620	-0.0913	3.1060	3.4931	83.2757	-0.0475	-0.1472
2.2633	1.8428	80.1039	0.7881	0.0861	3.1514	3.5335	69.9312	-0.1129	-0.1283
1.7475	2.1864	105.0564	0.7853	-0.0936	3.1410	2.7594	69.0297	0.2154	0.1170
3.0404	1.8176	68.8746	0.6361	0.2398	2.7137	3.1010	84.1779	0.2757	-0.1350
1.8469	3.5344	79.7372	0.6393	-0.2411	3.8316	2.7000	62.2144	-0.0489	0.3350
1.7340	1.5689	155.7917	0.6226	-0.0373	2.7767	4.3051	69.4277	-0.2263	-0.4784
3.0321	1.7108	113.4446	0.6043	0.2458	2.6385	2.4863	111.6218	0.5042	0.0611
3.0211	2.5837	128.5747	0.2711	0.1058	3.8766	2.7137	90.0550	-0.0359	0.4575
2.0613	3.6510	61.6408	0.4433	-0.2778	1.7420	2.9029	96.1294	0.6027	-0.2125
					3.8967	3.5109	100.6477	-0.3207	0.1664
					2.8829	4.3743	56.8361	-0.3318	-0.4079

Table 3. Expansion coefficients for the P(4,6) function of the $^1A_1$ state of He_2S^{2+}

All entries are in atomic units. The notation 3.650-05 represents 3.650 x 10^{-5}

Expansion basis function	Numerator	Denominator	Expansion basis function	Denominator
1	-4.0224+02	1.0000+00	$\rho_1^4\rho_2 + \rho_2^4\rho_1$	-6.3524-04
$\rho_1 + \rho_2$	-3.5866+02	-8.9165-01	$\rho_1^4\rho_3 + \rho_2^4\rho_3$	1.2708-03
ρ_3	-2.2321+02	-5.5492-01	$\rho_1\rho_3^4 + \rho_2\rho_3^4$	1.2075-03
$\rho_1^2 + \rho_2^2$	-8.1947+02	-2.0381+00	$\rho_1^3\rho_2^2 + \rho_1^2\rho_2^3$	3.1744-03
ρ_3^2	-2.4614+02	-6.1224-01	$\rho_1^3\rho_3^2 + \rho_2^3\rho_3^2$	1.8322-03
$\rho_1\rho_2$	-5.3595+01	-1.3337-01	$\rho_1^2\rho_3^3 + \rho_2^2\rho_3^3$	-1.9207-03
$\rho_2\rho_3 + \rho_1\rho_3$	-5.6965+02	-1.4159+00	$\rho_1^3\rho_2\rho_3 + \rho_1\rho_2^3\rho_3$	-1.0577-04
$\rho_1^3 + \rho_2^3$	-9.4467+02	-2.3472+00	$\rho_1\rho_2\rho_3^3$	-4.0259-03
ρ_3^3	-8.1392+01	-2.0216-01	$\rho_1^2\rho_2^2\rho_3$	-6.9217-03
$\rho_1^2\rho_2 + \rho_2^2\rho_1$	6.2972+01	1.5615-01	$\rho_1^2\rho_2\rho_3^2 + \rho_1\rho_2^2\rho_3^2$	3.4969-03
$\rho_1^2\rho_3 + \rho_2^2\rho_3$	-3.5781+02	-8.9039-01	$\rho_1^6 + \rho_2^6$	-2.0681-03
$\rho_1\rho_3^2 + \rho_2\rho_3^2$	-1.3892+02	-3.4505-01	ρ_3^6	-6.0920-05
$\rho_1\rho_2\rho_3$	-3.1015+02	-7.7216-01	$\rho_1^5\rho_2 + \rho_2^5\rho_1$	2.9120-03
$\rho_1^4 + \rho_2^4$	-4.6385+02	-1.1544+00	$\rho_1^5\rho_3 + \rho_2^5\rho_3$	-3.4069-03
ρ_3^4	-2.3456+02	-5.8353-01	$\rho_1\rho_3^5 + \rho_2\rho_3^5$	1.0124-03
$\rho_1^3\rho_2 + \rho_2^3\rho_1$	-2.0761+02	-5.1506-01	$\rho_1^4\rho_2^2 + \rho_2^4\rho_1^2$	-6.4950-03
$\rho_1^3\rho_3 + \rho_2^3\rho_3$	-9.7496+01	-2.4249-01	$\rho_1^4\rho_3^2 + \rho_2^4\rho_3^2$	5.8146-03
$\rho_1\rho_3^3 + \rho_2\rho_3^3$	2.6786+02	6.6647-01	$\rho_1^2\rho_3^4 + \rho_2^2\rho_3^4$	-4.2924-03
$\rho_1^2\rho_2^2$	2.8585+02	7.0586-01	$\rho_1^4\rho_2\rho_3 + \rho_2^4\rho_1\rho_3$	-1.1244-02
$\rho_1^2\rho_3^2 + \rho_2^2\rho_3^2$	-2.1785+02	-5.4264-01	$\rho_1^3\rho_2^3$	-6.7753-03
$\rho_1^2\rho_2\rho_3 + \rho_1\rho_2^2\rho_3$	1.7377+02	4.3341-01	$\rho_1\rho_2\rho_3^4$	5.2142-04
$\rho_1\rho_2\rho_3^2$	-1.4392+02	-3.6010-01	$\rho_1^3\rho_3^3 + \rho_2^3\rho_3^3$	-8.7760-04
$\rho_1^5 + \rho_2^5$		1.6516-03	$\rho_1^3\rho_2^2\rho_3 + \rho_1^2\rho_2^3\rho_3$	1.7233-02
ρ_3^5		4.4891-04	$\rho_1^3\rho_2\rho_3^2 + \rho_1\rho_2^3\rho_3^2$	5.5435-04
$(\chi^2)^{1/2}/E_h$	3.650-05			

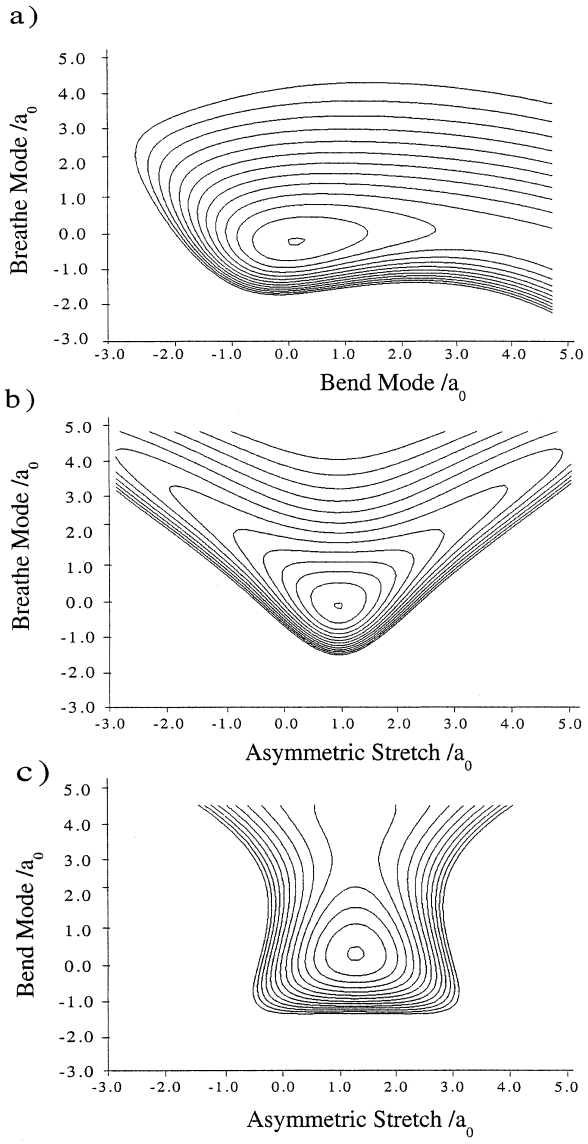

Fig. 1. Two-dimensional constant energy plots in terms of the normal coordinates for the $P(4, 6)$ potential energy function of He_2S^{2+}.

analytical functional form was the Ogilvie $P(4,6)$, provided that the singular values σ_{62}, σ_{65}, σ_{67} and s_{69-71} were set to zero. The coefficients of the fit are given in Table 3 [with a $(\chi^2)^{1/2}$ of 3.65×10^{-5} E_h]. Whilst this potential function was not the 'best' in terms of the 'goodness-of-fit', it yielded the lowest $(\chi^2)^{1/2}$ that was 'artefact-free'. That is, it contained no singularities or oscillations and so conformed to the anticipated physical properties of the analytical hypersurface. Fig. 1 gives three two-dimensional constant potential energy plots for the Ogilvie $P(4,6)$ potential function.

Table 4. Expansion coefficients of the dipole moment function of He_2O^{2+} and He_2S^2

All units in are ea_0. The notation 3.6786-02 represents 3.6786×10^{-2}

He_2O^{2+}				He_2S^{2+}			
μ_y ($C_{ijk} = C_{jik}$)		μ_x ($C_{ijk} = -C_{jik}$)		μ_y ($C_{ijk} = C_{jik}$)		μ_x ($C_{ijk} = -C_{jik}$)	
C_{000}	6.7405-01	C_{100}	2.3415-01	C_{000}	9.3326-02	C_{100}	3.4779-01
C_{100}	-2.8927-01	C_{200}	2.2902-02	C_{100}	-4.2366-01	C_{200}	3.9628-02
C_{001}	-2.8672-03	C_{101}	2.5135-03	C_{001}	1.8552-03	C_{101}	3.4077-03
C_{200}	7.6482-02	C_{300}	-1.2193-01	C_{200}	-3.1219-03	C_{300}	-4.9843-02
C_{110}	-6.5733-02	C_{210}	2.6782-03	C_{110}	-2.9156-02	C_{210}	4.6054-04
C_{101}	-4.2617-04	C_{201}	-2.7861-03	C_{101}	7.6191-04	C_{201}	2.9432-04
C_{002}	-1.0390-04	C_{102}	-3.6948-06	C_{002}	-8.9263-05	C_{102}	4.7175-05
C_{300}	5.0258-02	C_{400}	7.3467-02	C_{300}	3.4738-02	C_{400}	1.2165-02
C_{210}	1.0755-01	C_{310}	-2.3176-02	C_{210}	1.0845-02	C_{310}	6.3289-03
C_{201}	3.2307-03	C_{301}	-1.0687-02	C_{201}	-7.1129-04	C_{301}	-5.6139-04
C_{111}	1.4057-03	C_{211}	-6.4650-03	C_{111}	9.5019-04	C_{211}	-8.8072-04
C_{102}	5.4344-06	C_{202}	-1.7406-04	C_{102}	5.7747-05	C_{202}	-2.2946-05
C_{003}	7.5333-07	C_{103}	-1.2590-06	C_{003}	1.1349-06	C_{103}	-3.6165-07
C_{400}	-2.4410-02	C_{500}	-4.0596-02	C_{400}	-1.4546-02	C_{500}	-1.9095-03
C_{310}	-1.7860-02	C_{410}	1.3060-02	C_{310}	-8.1639-03	C_{410}	-4.4877-03
C_{220}	6.2285-02	C_{320}	-6.5064-02	C_{220}	-1.2996-02	C_{320}	7.5484-04
C_{301}	-2.1635-04	C_{401}	6.4804-03	C_{301}	-8.2773-04	C_{401}	-9.7003-06
C_{211}	-1.3547-03	C_{311}	5.4043-03	C_{211}	1.2875-03	C_{311}	-3.4448-04
C_{202}	5.4683-05	C_{302}	1.8680-04	C_{202}	3.5344-05	C_{302}	-3.7890-06
C_{112}	1.0138-04	C_{212}	9.1897-05	C_{112}	-2.8743-04	C_{212}	5.8079-05
C_{103}	-3.4822-07	C_{203}	4.9462-06	C_{103}	-3.6601-07	C_{203}	1.0885-07
C_{004}	1.7135-09	C_{104}	4.3147-08	C_{004}	-1.9810-08	C_{104}	-8.5837-09
C_{500}	1.1008-02			C_{500}	1.0732-02		
C_{410}	-2.6083-02			C_{410}	3.7603-03		
C_{320}	1.2571-02			C_{320}	6.9691-03		
C_{401}	2.7717-04			C_{401}	1.8703-03		
C_{311}	2.5110-03			C_{311}	-1.9842-03		
C_{221}	-2.3831-03			C_{221}	1.8284-03		
C_{302}	-7.1417-05			C_{302}	-4.4176-04		
C_{212}	-7.3424-05			C_{212}	8.5371-05		
C_{203}	-1.8733-06			C_{203}	8.0335-07		
C_{113}	-2.9673-07			C_{113}	1.1076-04		
C_{104}	1.8279-08			C_{104}	4.8637-07		
C_{005}	-9.5677-11			C_{005}	2.0104-09		
				C_{600}	1.9295-03		
				C_{510}	1.0099-03		
				C_{420}	-5.0002-04		
				C_{330}	2.3888-03		
				C_{501}	-5.0028-05		
				C_{411}	-2.9121-04		

Table 4 (*Continued*)

He_2O^{2+}		He_2S^{2+}		
μ_y ($C_{ijk} = C_{jik}$)	μ_x ($C_{ijk} = -C_{jik}$)	μ_y ($C_{ijk} = C_{jik}$)		μ_x ($C_{ijk} = -C_{jik}$)
		C_{321}	1.1240-03	
		C_{402}	4.4107-04	
		C_{312}	8.3002-04	
		C_{222}	-4.9449-04	
		C_{303}	8.9336-06	
		C_{213}	-4.0026-05	
		C_{204}	-1.4911-06	
		C_{114}	4.5127-08	
		C_{105}	-1.6813-08	
		C_{006}	-8.7212-11	
		C_{700}	-3.1588-03	
		C_{610}	-2.6984-03	
		C_{520}	-2.4348-03	
		C_{430}	6.1954-04	
		C_{601}	4.9723-04	
		C_{511}	1.2237-03	
		C_{421}	-1.2348-03	
		C_{331}	1.3588-03	
		C_{502}	5.1839-04	
		C_{412}	9.1959-05	
		C_{322}	-1.1192-03	
		C_{403}	3.2552-05	
		C_{313}	-7.7130-05	
		C_{223}	-2.2762-04	
		C_{304}	2.6507-06	
		C_{214}	-2.9223-06	
		C_{205}	6.1654-08	
		C_{115}	-9.2489-08	
		C_{106}	1.6654-10	
		C_{007}	8.6985-13	
$(\chi^2)^{1/2} = 3.6786\text{-}02$	$(\chi^2)^{1/2} = 9.4542\text{-}03$	$(\chi^2)^{1/2} = 1.8826\text{-}04$		$(\chi^2)^{1/2} = 3.0888\text{-}04$

The DMS for H_2O is available from E-PAPS (1997). It was constructed from the product of the point charge and the position vectors in a conveniently orientated coordinate system (PS 1997). The point charge function is a scalar function, expanded in terms of Legendre polynomials and a many-bodied term (PS 1997).

Previously, we have constructed the DMS of a number of triatomic molecules as a power series expansion in the terms of the three normal coordinates (Searles and von Nagy-Felsobuki 1988, 1991, 1992, 1993). Such a procedure was useful in evaluating vibrational transition probability integrals using Gauss quadrature schemes. However, errors in the fit far exceeded the calculated errors of individual points on the dipole moment hypersurface (Searles and von Nagy-Felsobuki 1988, 1991, 1992, 1993). In order to generate a more accurate DMS, we have employed a functional form as outlined by Gabriel *et al.* (1993). Their dipole function is given in terms of displacement coordinates in a power series expansion of bond lengths ($Q_{1,2} = r_i - r_e$) and the included bond angle

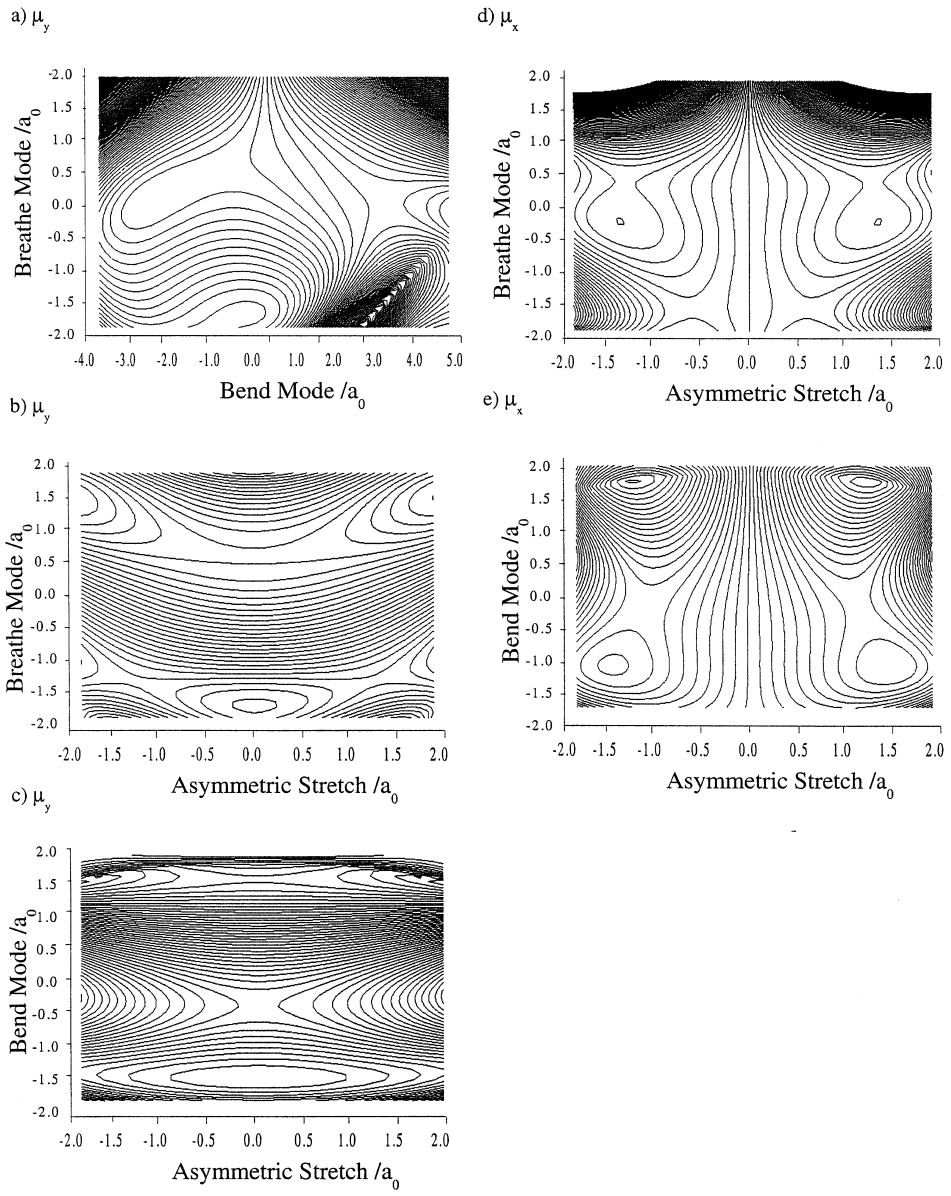

Fig. 2. Two-dimensional constant dipole plots in terms of the normal coordinates for the fifth order dipole moment function of He_2O^{2+}: (a)–(c) μ_y and (d), (e) μ_x.

($Q_3 = \alpha_i - \alpha_e$). Here the labels 'i' refer to the individual instantaneous bond lengths and bond angle, whereas the labels 'e' denotes the equilibrium values. The Cartesian coordinates were such that the x coordinate bisected the included bond angle.

For He_2O^{2+} and He_2S^{2+}, the (r_e, α_e) geometry was ($2.2076a_0$, 92.6°) and ($3.1188a_0$, 76.6°) respectively. The analytical function for He_2O^{2+} (He_2S^{2+}) was defined within the range of $1.1471a_0$ ($1.7420a_0$) $\leq r_{He–O(S)} \leq 3.0765a_0$ ($4.3743a_0$) and 33.9° (37.4°) $\leq \alpha_{He–O(S)–He} \leq 138.8°$ respectively. Table 4 gives the expansion coefficients for each

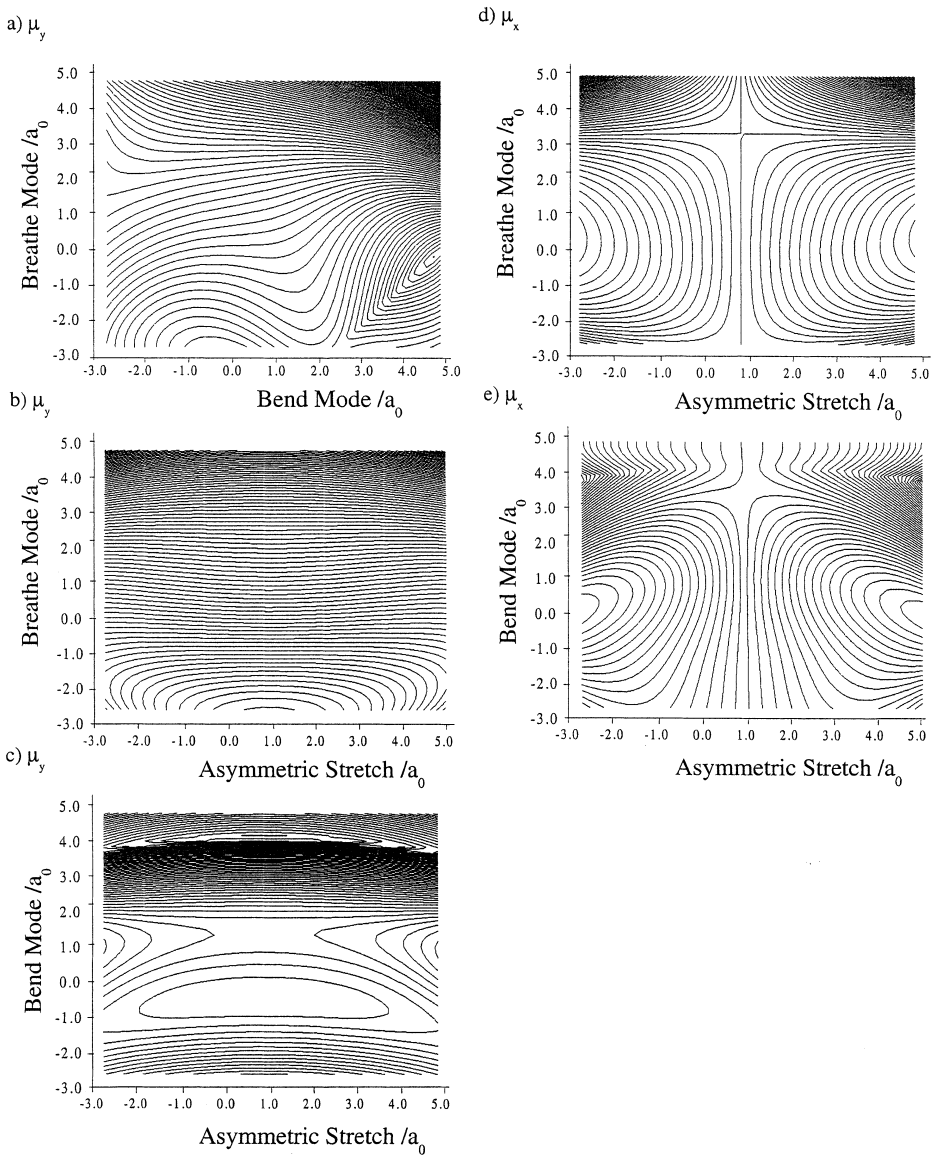

Fig. 3. Two-dimensional constant dipole plots in terms of the normal coordinates for the dipole moment function of He_2S^{2+}: (a)–(c) fourth order for μ_y and (d), (e) fifth order for μ_x.

component of the dipole moment function of He_2O^{2+} and He_2S^{2+}. For the μ_x component, a fifth order power series expansion was used respectively, whereas for the μ_y component a fifth and fourth order power series expansion was used respectively for both the helides. The $(\chi^2)^{1/2}$ for fits are at least three orders of magnitude smaller than what was previously achievable using a normal coordinate expansion for triatomic molecules (see e.g. Searles and von Nagy-Felsobuki 1988, 1991, 1992, 1993). Figs 2 and 3 give the contour plots in terms of their normal coordinates of each component of the dipole moment function for He_2O^{2+} and He_2S^{2+} respectively.

4. Ro–vibrational Transition Energies

The vibrational Hamiltonian used in all subsequent calculations is the **t** coordinate Hamiltonian derived by Carney *et al.* (1977). The rectilinear Hamiltonian has the form

$$H = T_V + T_I + U_W + V\,, \tag{1}$$

where the first term is the vibrational kinetic energy operator, the second term is the vibrational angular momentum operator, the third term is the Watson operator and the last term is the potential energy operator.

The basic approach that we have adopted for the variational solution of the corresponding eigenvalue problem of equation (1) has been detailed by Doherty *et al.* (1986) and Searles and von Nagy-Felsobuki (1988, 1991, 1993). It differs vastly from the variational approach used by PS (1997). They employed a Radau hyperspherical Hamiltonian with self-consistent-field nodeless vibration configuration basis functions and also analytical integrations for all integrals except the potential energy integrator for which they use a Gauss–Legendre quadrature scheme.

To further emphasise the differences in the two solution algorithms, the following points need to be made about our approach. The one-dimensional wave functions are calculated using a finite-element solution of a one-dimensional Hamiltonian, which is expressed in terms of a single **t** coordinate. For each **t** coordinate 1000 finite-elements are constructed within each domain. A 'full' $20 \times 20 \times 20$ three-dimensional configuration basis was spliced from the one-dimensional solutions, yielding an 8000 size basis set for use in the variational solution of the three-dimensional problem. For the three-dimensional Hamiltonian, a third-order expansion of the Watson operator was used. The potential energy integrals were evaluated using the HEG (1965) scheme, whereas all other integrals were evaluated using a sixteen point Gauss quadrature scheme. Finally, the secular determinant was constructed using equation (1), spanned by the configuration basis set and then diagonalised to yield vibrational wave functions and eigenenergies (both of which are required for the ro–vibrational problem).

Table 5 compares the experimental vibrational band origins (VBO) of H_2O with the variational solutions of PS (1997) and those obtained using our algorithm. It should be noted that both calculations used the same PES. The agreement between the two calculations, and with experiment, is excellent. The lowest twenty VBO yield identical assignments (with our assignments being based on the expansion densities of the configurational basis functions in the wave function). The difference between our calculated result and that of PS (1997) is within 1.0 cm^{-1} for all the low-lying VBO, except for those assigned as the excited states of the bend mode. Our calculated results for the excited bend modes below 6200 cm^{-1} are in excellent agreement with experiment and with PS (1997). However, for the $\langle 050 \rangle$ and $\langle 060 \rangle$ VBO our calculated results are in poorer agreement with the experimental values (Zobov *et al.* 1999) than those of PS (1997). This suggests that the limitations we have imposed on the truncation of our basis set (i.e. 8000 basis functions) have been too severe for these highly excited bend modes.

Table 5 also compares the vibrational band origins of H_2O, He_2O^{2+} and He_2S^{2+}. The VBO display the expected trends associated with their reduced mass. Table 5 also gives the expansion densities for the dominant configurational component. From these densities it is clear that the wave functions are not diagonal in terms of the configurational basis functions. This is due to the Hamiltonian, which has embedded in it the 'full' mechanical anharmonicity as well as operators that couple the **t** vibrational modes. Hence,

Table 5. Assignment and comparison of the VBO of H_2O, He_2O^{2+} and He_2S^{2+} (in cm^{-1})

H_2O							He_2O^{2+}			He_2S^{2+}		
This work [a]			Theory [b]		Experiment [c]		This work [d]			This work [d]		
$t_1t_2t_3$	Density	VBO	VBO	Δ_1	VBO	Δ_2	$t_1t_2t_3$	Density	VBO	$t_1t_2t_3$	Density	VBO
|000>	1.00	0.0	0.0	0.0	0.0	0.0	|000>	0.95	0.0	|000>	0.97	0.0
|010>	1.0	1594.9	1594.8	0.1	1594.7	0.2	|010>	0.69	816.8	|010>	0.90	330.9
|020>	1.0	3152.0	3151.6	0.4	3151.6	0.4	|100>	0.68	1242.3	|001>	0.87	612.4
|100>	1.0	3657.1	3657.0	0.1	3657.1	0.0	|001>	0.84	1275.6	|100>	0.46	618.0
|001>	1.0	3756.0	3756.0	0.0	3755.9	0.1	|020>	0.43	1595.9	|020>	0.44	637.9
|030>	1.0	4667.7	4666.8	0.9	4666.8	0.9	|020>	0.29	2038.9	|030>	0.66	890.5
|110>	1.0	5235.2	5235.0	0.2	5235.0	0.2	|011>	0.59	2042.4	|011>	0.77	919.5
|011>	1.0	5331.3	5331.2	0.1	5331.3	0.0	|030>	0.19	2339.0	|110>	0.70	949.2
|040>	0.9	6136.1	6134.0	2.1	6134.0	2.1	|200>	0.35	2438.8	|040>	0.55	1111.9
|120>	0.9	6775.5	6775.1	0.4	6775.1	0.4	|101>	0.43	2458.5	|101>	0.29	1179.1
|021>	1.0	6871.8	6871.5	0.3	6871.5	0.3	|002>	0.59	2526.8	|002>	0.41	1180.2
|200>	0.9	7201.6	7201.5	0.1	7201.5	0.1	|021>	0.34	2774.1	|021>	0.38	1201.5
|101>	0.9	7249.9	7249.9	0.0	7249.8	0.1	|030>	0.32	2798.3	|050>	0.23	1226.4
|002>	0.9	7445.2	7445.1	0.1	7445.1	0.1	|030>	0.20	3047.1	|120>	0.24	1231.1
|050>	0.9	7547.9	7542.5	5.4	7542.4 [e]	5.5	|012>	0.19	3199.0	|200>	0.57	1252.8
|130>	0.9	8275.0	8274.0	1.0	8274.0	1.0	|021>	0.25	3204.9	|050>	0.42	1275.1
|031>	0.9	8374.6	8373.9	0.7	8373.9	0.7	|012>	0.27	3264.2	|060>	0.53	1355.6
|210>	0.8	8761.9	8761.7	0.2	8761.6	0.3	|021>	0.19	3471.9	|031>	0.46	1425.6
|111>	0.9	8807.2	8807.0	0.2	8807.0	0.2	|040>	0.25	3522.0	|070>	0.45	1446.0
|060>	0.8	8885.7	8870.6	15.1	8870.5 [e]	15.2	|202>	0.16	3578.9	|012>	0.30	1466.9

[a] Using the solution algorithm of Searles and von Nagy-Felsobuki (1988, 1991, 1993), but also incorporating the PES and DMS of PS (1997).

[b] See Partridge and Schwenke (1997). Note that $\Delta_1 = \left|\mathrm{VBO}_{\text{This work}} - \mathrm{VBO}_{\text{PS}}\right|$.

[c] See Rothman *et al.* (1998). Note that $\Delta_2 = \left|\mathrm{VBO}_{\text{This work}} - \mathrm{VBO}_{\text{Exp}}\right|$.

[d] Using the solution algorithm of Searles and von Nagy-Felsobuki (1988, 1991, 1993).

[e] See Zobov *et al.* (1999).

Table 6. Low-lying rotational energy levels of the ground vibration of H_2O, He_2O^{2+} and He_2S^{2+}

Note that $\Delta = |E_{rot}(\text{This work}) - E_{rot}(\text{PS})|$

J	K_a	K_c	$R^{\pm}_{JKM}$	Density	$E_{rot}(\Delta)$ (cm^{-1})
			(a) H_2O		
0	0	0	0	1.00	0.0 (0.0)
1	0	1	-1	1.00	23.8(0.0)
1	1	1	1	1.00	37.0(0.1)
1	1	0	0	1.00	42.3(0.1)
2	0	2	2	0.86	70.0(0.0)
2	1	2	-2	1.00	79.4(0.1)
2	1	1	-1	1.00	95.0(0.1)
2	2	1	1	1.00	134.5(0.4)
2	2	0	0	0.86	135.8(0.4)
3	0	3	-3	0.87	136.7(0.1)
3	1	3	3	0.97	142.1(0.1)
3	1	2	2	0.71	173.1(0.2)
3	2	2	-2	1.00	205.8(0.4)
3	2	1	-1	0.87	211.7(0.4)
3	3	1	1	0.97	284.3(0.9)
3	3	0	0	0.71	284.5(0.9)
4	0	4	4	0.90	221.9(0.1)
4	1	4	-4	0.95	224.7(0.2)
4	1	3	-3	0.63	275.2(0.3)
4	2	3	3	0.92	299.8(0.5)
4	2	2	2	0.54	315.3(0.5)
4	3	2	-2	0.95	381.6(0.9)
4	3	1	-1	0.63	382.9(0.9)
4	4	1	1	0.92	486.6(1.5)
4	4	0	0	0.61	486.6(1.5)
			(b) He_2O^{2+}		
0	0	0	0	1.00	0.0
1	0	1	-1	1.00	4.6
1	1	1	1	1.00	6.6
1	1	0	0	1.00	7.7
2	0	2	2	0.94	13.5
2	1	2	-2	1.00	14.8
2	1	1	-1	1.00	18.0
2	2	1	1	1.00	23.9
2	2	0	0	0.94	24.2
3	0	3	-3	0.95	26.2
3	1	3	3	0.99	26.8
3	1	2	2	0.86	33.2
3	2	2	-2	1.00	37.8
3	2	1	-1	0.95	39.3
3	3	1	1	0.99	50.5
3	3	0	0	0.86	50.6
4	0	4	4	0.97	42.4
4	1	4	-4	0.98	42.6
4	1	3	-3	0.83	52.9
4	2	3	3	0.96	56.0
4	2	2	2	0.76	59.8
4	3	2	-2	0.98	69.5
4	3	1	-1	0.83	69.9
4	4	1	1	0.96	86.6
4	4	0	0	0.80	86.6

Table 6 (*Continued*)

J	K_a	K_c	$R^{\pm}_{JKM}$	Density	$E_{rot}(\Delta)$ (cm^{-1})
			(c) He_2S^{2+}		
0	0	0	0	1.00	0.0
1	0	1	-1	1.00	2.4
1	1	1	1	1.00	2.8
1	1	0	0	1.00	3.5
2	0	2	2	0.99	6.8
2	1	2	-2	1.00	6.9
2	1	1	-1	1.00	9.1
2	2	1	1	1.00	10.1
2	2	0	0	0.99	10.6
3	0	3	-3	0.99	12.9
3	1	3	3	1.00	12.9
3	1	2	2	0.95	16.9
3	2	2	-2	1.00	17.4
3	2	1	-1	0.99	19.1
3	3	1	1	1.00	21.2
3	3	0	0	0.95	21.4
4	0	4	4	1.00	20.6
4	1	4	-4	1.00	20.6
4	1	3	-3	0.97	26.6
4	2	3	3	0.99	26.7
4	2	2	2	0.89	30.2
4	3	2	-2	1.00	31.4
4	3	1	-1	0.97	32.6
4	4	1	1	0.99	36.0
4	4	0	0	0.99	36.1

configurational basis functions that belong to the same irreducible representations may mix. This complicates the comparison of the assignments. For example, the fifth and six wave functions of He_2O^{2+} are dominated by the same configurational components, namely ($|020\rangle$, $|110\rangle$), with the expansion densities of size (0.43, 0.12) and (0.30, 0.27) respectively. In order to simplify the assignments it would be more appropriate to use the irreducible representation classification. Thus, only those configurations with an odd quanta in the asymmetric stretch mode, belong to the B_2 irreducible representation, with all other configurations having A_1 symmetry.

In the case of H_2O the expansion densities are greater than 0.8 for all the low-lying VBO, whereas for He_2O^{2+} and He_2S^{2+} this is only achieved for four and six VBO respectively. According to the symmetry classification, the assignments of He_2O^{2+} and He_2S^{2+} are similar (differing only in the order of the third and fourth wave function and the assignment of the sixteenth). In the case of H_2O, the curvature of the potential for the asymmetric stretch coordinate is far steeper than for either He_2O^{2+} or He_2S^{2+}, thereby yielding a significantly different assignment.

The ro–vibrational Hamiltonian in the vibration matrix representation as given by Carney *et al.* (1977) has the form

$$H^{RV}_{ij} = E_i\langle S\rangle_{ij} + 0.5\langle A\rangle_{ij}\Pi_x^2 + 0.5\langle B\rangle_{ij}\Pi_y^2 + 0.5\,\langle C\rangle_{ij}\Pi_z^2 + 0.5\langle D\rangle_{ij}(\Pi_x\Pi_y + \Pi_y\Pi_x) + \tfrac{i}{\hbar}\langle F\rangle_{ij}\Pi_z\,, \tag{2}$$

where E_i is the i^{th} pure vibrational eigenenergy, $\langle S\rangle_{ij}$ is the vibration overlap matrix element and Π are the angular momentum operators whose components are referred to the

molecule-fixed coordinate system. The vibration-averaged rotational constants are labelled $\langle A\rangle_{ij}$, $\langle B\rangle_{ij}$, $\langle C\rangle_{ij}$ and $\langle D\rangle_{ij}$. The matrix element $\langle F\rangle_{ij}$ is the Coriolis coupling term.

The full ro–vibrational wave function $\Psi(\nu, r)$ is given by a linear combination of a configurational basis composed of vibrational wave functions $\psi(\nu)$ (solutions of equation 1) and symmetric-top functions Φ_{jkm}. To ensure that the Hamiltonian matrix representation contained real matrix elements, plus and minus combinations of regular symmetric-top eigenfunctions $R^{\pm}_{jkm}$ were used, namely

$$\Psi_{VJKM} = \sum_{V=1}^{NV}\left[\sum_{K=J}^{K=1} C_{VJKm}\psi_V R^{-}_{JKM} + C_{VJ0M}\psi_V \Phi_{J0M} + \sum_{K=1}^{K=J} C_{VJKp}\psi_V R^{+}_{JKM}\right],$$

$$R^{-}_{JKM} = \frac{1}{\sqrt{2i}}\left(\Phi_{JKM} - \Phi_{J(-K)M}\right),$$

$$R^{+}_{JKM} = \frac{1}{\sqrt{2}}\left(\Phi_{JKM} + \Phi_{J(-K)M}\right). \tag{3}$$

Carney *et al.* (1977) have detailed the matrix elements spanned by plus and minus combinations of the regular top eigenfunctions incorporating the angular momentum operators. The H^{RV} matrix is constructed using the ro–vibrational configurational basis set and is diagonalised yielding ro–vibrational eigenenergies and eigenfunctions.

Table 6 compares the low-lying rotational energy levels of the ground vibrational state for the $^1A_1$ state of H_2O, He_2O^{2+} and He_2S^{2+}. Our calculation predicts that the ground vibrational state of H_2O is 4638.0 cm^{-1}, which is the same as that calculated by PS (1997). The largest discrepancy between the two solution algorithms is 1.5 cm^{-1}, which occurs for the highest J level compared. The rotational levels for He_2O^{2+} and He_2S^{2+} show the expected trend due to their increasing reduced mass.

5. Ro–vibrational Transition Probabilities

A novel approach for the numerical calculation of three-dimensional vibration transition moment integrals is to employ the HEG (1965) quadrature scheme. These integrals are given by

$$\langle\psi_i(t_1)\psi_j(t_2)\psi_k(t_3)|\mu_p|\psi_l(t_1)\psi_m(t_2)\psi_n(t_3)\rangle = \langle ijk|\mu_p|lmn\rangle\,, \tag{4}$$

where the ψ are the one-dimensional wave functions dependent on one of the **t** coordinates and p labels the Cartesian components of the dipole moment operator in the molecule-fixed framework. Assuming that the dipole moment operator can be expanded as a convergent power series in the normal coordinates t_1, t_2 and t_3, equation (4) then becomes

$$\langle ijk|\mu_p|lmn\rangle = \langle ijk|c_0|lmn\rangle + i\langle ijk|c_1t_1|lmn\rangle + j\langle ijk|c_2t_2|lmn\rangle + k\langle ijk|c_3t_3|lmn\rangle + \ldots$$

$$\text{higher-order terms.} \tag{5}$$

Truncating to first order, the transition probability integral becomes

$$\langle ijk|\mu_p|lmn\rangle = c_0\delta_{il}\delta_{jm}\delta_{kn} + ic_1\delta_{jm}\delta_{kn}X_{il}(t_1) + jc_2\delta_{il}\delta_{kn}X_{jm}(t_2) + kc_3\delta_{il}\delta_{jm}X_{kn}(t_3)\,, \tag{6}$$

where the elements of the matrix $X_{il}(t_q)$ for each coordinate are given by

$$X_{il}(t_q) = \langle\psi_i(t_q)|t_q|\psi_l(t_q)\rangle\,. \tag{7}$$

Table 7. Vibration transition frequencies, square dipole matrix elements, Einstein coefficients, band strengths and radiative lifetimes for H_2O, He_2O^{2+} and He_2S^{2+}

Square dipole moment and band strengths are calculated at 296 K
The notation 1.62+05 represents $1.62 \times 10^{+5}$

j	i	ν_{ji} (cm^{-1})	R^2 (au^2)	A_{ji} (s^{-1})	S_{ji} (cm $molecule^{-1}$)	τ [a] (s)
			(a) H_2O			
1	0	1594.9	1.80-02	2.34+01	1.24-17	0.04
2	0	3152.0	6.70-05	6.54-01	8.85-20	0.02
3	0	3657.1	3.10-04	4.73+00	4.76-19	0.17
4	0	3756.0	5.90-03	9.73+01	9.27-18	0.01
5	0	4667.7	2.70-07	8.59-03	5.30-22	0.01
6	0	5235.2	6.80-06	3.07-01	1.51-20	0.03
7	0	5331.3	3.30-04	1.56+01	7.40-19	0.01
8	0	6136.1	1.00-09	7.28-05	2.60-24	0.01
9	0	6775.5	7.30-07	7.11-02	2.08-21	0.02
10	0	6871.8	1.40-05	1.38+00	3.93-20	0.01
			(b) He_2O^{2+}			
1	0	816.9	7.1-02	1.21+01	2.31-17	5.68-02
2	0	1242.4	1.6-01	9.91+01	8.28-17	9.71-03
3	0	1275.7	1.5+00	9.49+02	7.53-16	1.04-03
4	0	1596.1	3.2-04	4.03-01	2.05-19	3.22-02
5	0	2039.1	8.5-03	2.26+01	7.04-18	6.31-03
6	0	2042.7	6.3-02	1.69+02	5.25-17	6.70-04
7	0	2339.2	3.2-05	1.30-01	3.08-20	2.24-02
8	0	2439.1	1.9-02	8.77+01	1.91-17	1.91-03
9	0	2458.8	7.9-03	3.70+01	7.92-18	9.74-04
10	0	2527.1	7.4-04	3.76+00	7.62-19	5.89-04
			(c) He_2S^{2+}			
1	0	330.9	1.3+02	1.53+03	1.04-14	1.45-4
2	0	612.4	5.8-02	4.19+00	9.86-18	1.83-4
3	0	618.0	8.4+01	6.20+03	1.44-14	5.22-5
4	0	637.9	1.3+01	1.08+03	2.36-15	8.76-5
5	0	890.7	1.0+00	2.24+02	2.59-16	1.92-5
6	0	919.5	1.5-03	3.71-01	4.05-19	4.39-5
7	0	949.2	1.5+01	4.14+03	4.24-15	3.39-5
8	0	1112.3	2.5-01	1.07+02	8.04-17	8.16-6
9	0	1179.2	9.3-04	4.79-01	3.20-19	1.45-5
10	0	1180.2	3.1+02	1.62+05	1.08-13	4.11-6

[a] Lifetime of upper state.

Hence $X(t_q)$ gives the expectation of the normal coordinate. If $\mathbf{D}(t_q)$ is defined as the diagonal form of $X(t_q)$ and $C(t_q)$ are the eigenvectors, then $X(t_q)$ is expressed as

$$X(t_q) = (C(t_q))^T D(t_q) C(t_q) . \tag{8}$$

The diagonal elements of $X(t_q)$ are the quadrature points of t_q. The expectation values of $X(t_q)$ can be evaluated numerically and therefore the matrix can be diagonalised to determine the quadrature points in equation (9). The transition probability integrals are determined by evaluating the dipole moments at the quadrature points using the fitted DMS via

$$\langle \psi_i(t_1)\psi_j(t_2)\psi_k(t_3)|\mu_p(X(t_1)X(t_2)X(t_3))|\psi_l(t_1)\psi_m(t_2)\psi_n(t_3)\rangle =$$

$$C(t_1)C(t_2)C(t_3)\mu_p(D(t_1)D(t_2)D(t_3))(C(t_1))^T(C(t_2))^T(C(t_3))^T . \quad (9)$$

Table 7 gives the vibration transition frequencies, square dipole matrix elements, Einstein coefficients and radiative lifetimes for the $^1A_1$ state of H_2O, He_2O^{2+} and He_2S^{2+}. For molecules belonging to the C_{2v} symmetry there are no Raman forbidden transitons. Hence, lifetimes of the excited states for H_2O are small for transitions connected to the ground vibrational state. The longest lifetime of 11.4 s is for an excited state of He_2S^{2+} for an assigned wave function with expansion densities of the form: 0.55 $|040\rangle$ + 0.13 $|140\rangle$ + 0.11 $|030\rangle$ + 0.05 $|050\rangle$ + 0.04 $|060\rangle$. Similar lifetimes for highly excited states have been calculated for the alkali metal trimers (Searles and von Nagy-Felsobuki 1993).

The radiative transition probabilities (R^2) between the two ro–vibrational levels can be evaluated using (Zare 1987)

$$R^2 = \sum_{M_1} \sum_{M_2} |\langle \Psi_{V_1 J_1 K_1 M_1} | \mu_{SF} | \Psi_{V_2 J_2 K_2 M_2} \rangle|^2 , \quad (10)$$

where Ψ_{VJKM} is the ro–vibrational wave function and μ_{SF} is the dipole moment function in the space fixed (SF) framework. In this framework the dipole moment in the three spatial directions are equivalent and so the dipole moment operator in the equation (10) can be replaced with 3 μ_z.

Since the dipole moment operator was constructed within the molecule-fixed framework, it needs to be transformed into the SF framework via (Zare 1987)

$$\mu_z = \frac{1}{\sqrt{2}}[\mu_x(D^1_{0-1} - D^1_{01}) - i\mu_y(D^1_{0-1} + D^1_{01})] , \quad (11)$$

where μ_x and μ_y are the dipole moment components in molecule-fixed coordinates, and the D are the appropriate Wigner rotation matrices.

By using equations (3) and (11) the ro–vibrational transition probabilities can be derived as

$$R^2 = \frac{3}{8}\left[\frac{2J_1+1}{8\pi^2}\right]\left[\frac{2J_2+1}{8\pi^2}\right]\sum_{M_1}\sum_{M_2}\Bigg|\Bigg\langle\sum_{V=1}^{NV}\Bigg[\sum_{K_1=J_1}^{K_1=1} C_{V_1J_1Km_1}\psi_{V_1}(i(\Phi_{J_1K_1M_1} - \Phi_{J_1(-K_1)M_1}))$$

$$+ \sqrt{2}\, C_{V_1J_10_1M_1}\psi_{V_1}D^J_{M_10} + \sum_{K_1=1}^{K_1=J_1} C_{V_1J_1Kp_1}\psi_{V_1}(D^{J_1}_{M_1K_1} + D^{J_1}_{M_1-K_1})\Bigg]$$

$$\times\left|\left[\mu_x(D^1_{0-1} - D^1_{01}) - i\mu_y(D^1_{0-1} + D^1_{01})\right]\right|\sum_{V=2}^{NV}\Bigg[\sum_{K_2=J_2}^{K_2=1} C_{V_2J_2Mm_2}\psi_{V_2}(i(\Phi_{J_2K_2M_2} - \Phi_{J_2(-K_2)M_2}))$$

$$+ \sqrt{2}\, C_{V_2J_20_21M_2}\psi_{V_2}D^{J_2}_{M_20} + \sum_{K_2=1}^{K_2=J_2} C_{V_2J_2Kp_2}\psi_{V_2}(\Phi_{J_2K_2M_2} + \Phi_{J_2(-K_2)M_2})\Bigg]\Bigg\rangle\Bigg|^2 . \quad (12)$$

It should be noted that the rotational wave functions can be cast in terms of the Wigner rotational matrices (Zare 1987). Hence, integrals involving these rotation matrices $\langle D^{J_1}{}_{M_1K_1}\, D^1{}_{0-1}\, D^{J_2}{}_{M_2K_2}\rangle$ are evaluated analytically following the recipe given by Zare (1987). The three-dimensional vibration transition moment integrals are evaluated using the HEG (1965) scheme (see equation 4).

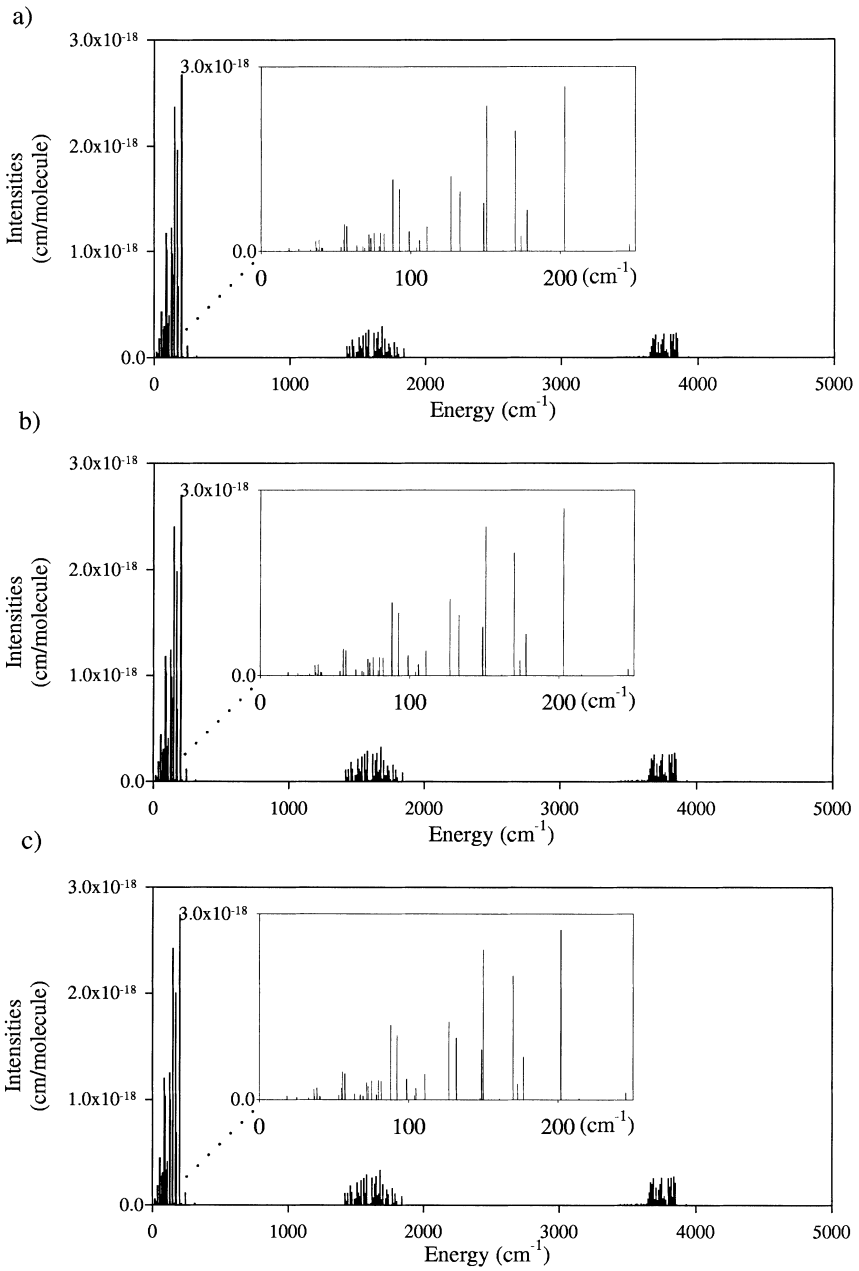

Fig. 4. Comparison of the ro–vibrational spectra of water for 819 transitions (up to and including the ν = 4 and J = 4 level). The insets are an expansion of the transitions between 0–250 cm^{-1}. (a) Experiment HITRAN (Rothman *et al.* 1998); (b) PS (1997); and (c) using the solution algorithm for Searles and von Nagy-Felsobuki (1988, 1991, 1993) but also incorporating the PES and DMS of PS (1997).

We have assigned all the ro–vibrational levels using our expansion density analysis. For the vibration–rotation states higher than the fourth excited rotational state, the resultant wave functions are heavily mixed and so the assignment of a state in terms of a single

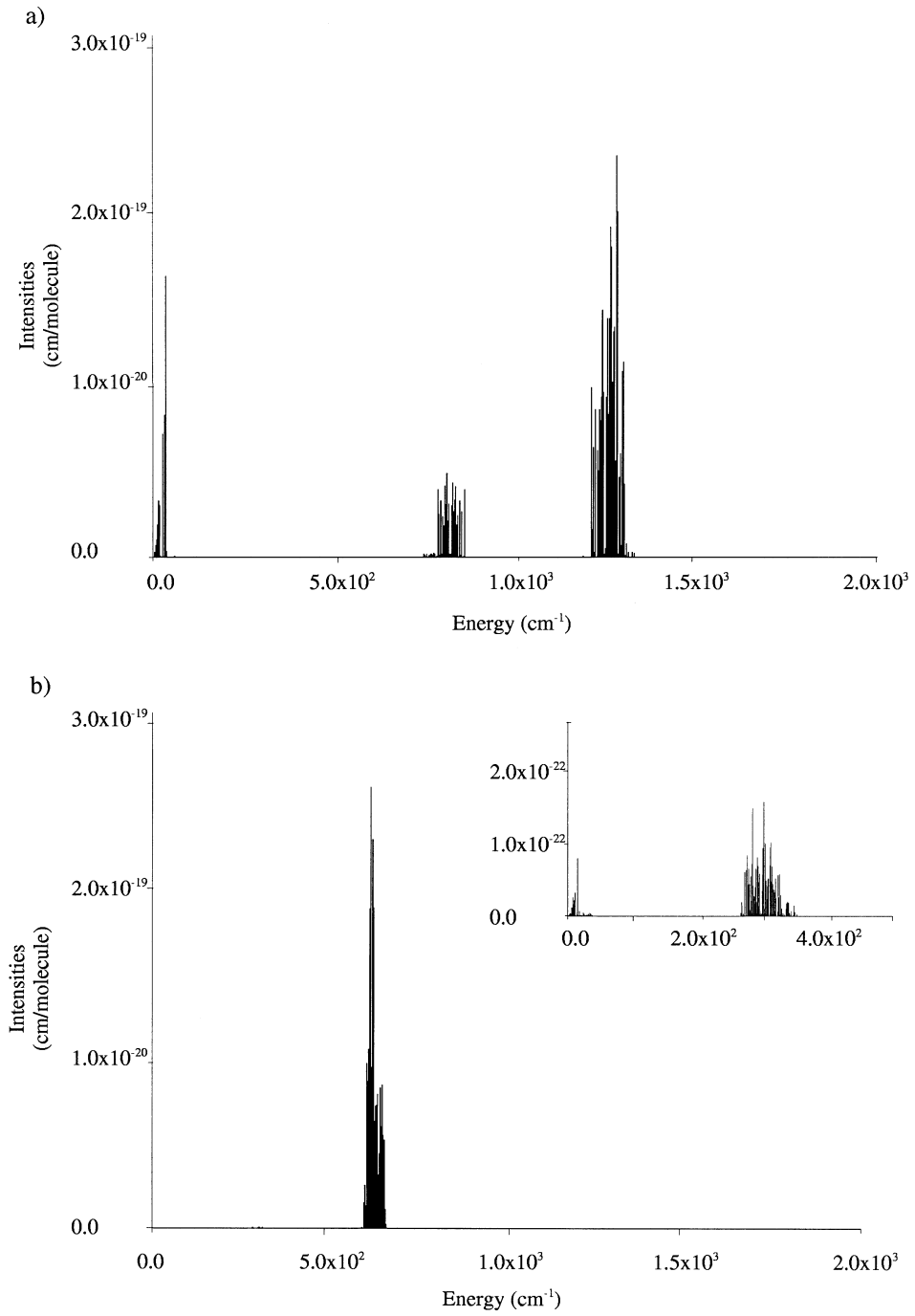

Fig. 5. Comparison of ab initio ro–vibrational spectra up to and including the $\nu = 4$ and $J = 4$ level using a line strength threshold of 1.0×10^{-30} cm per molecule: (a) He_2O^{2+} 634 transitions and (b) He_2S^{2+} 685 transitions.

diagonal representation becomes problematical. This is also evident in the published H_2O wave function of PS (1997). For example, the expansion density for the $|\nu_1 = 4, \nu_2 = 0, \nu_3 = 0\rangle \mid J = 4, K_a = 0, K_c = 4\rangle$ component is 0.22, whereas the other component contributing to the same PS wave function, namely $|\nu_1 = 3, \nu_2 = 0, \nu_3 = 2\rangle \mid J = 4, K_a = 0, K_c = 4\rangle$, has an expansion density of 0.21 (see E-PAPS 1997). Hence, to assign this rotational energy level to the former component and not the the latter is problematical (see the comments made by PS 1997). We have experienced a similar difficulty and so have restricted our analysis to energy levels whose wave functions (according to our expansion density analysis) have unequivocal assignments. That is, we have restricted our analysis to transitions, which are up to and which include, the $\nu = 4$ and $J = 4$ levels for H_2O, He_2O^{2+} and He_2S^{2+}.

According to the ro–vibrational selection rules the total number of allowable transitions up to and including the $\nu = 4$ and $J = 4$ levels is 1250. However, many of these line strengths are still not significant (i.e. well below 10^{-30} cm molecule^{-1}). There are only 819 transitions which have been assigned, up to and including the $\nu = 4$ and $J = 4$ level, in the experimental HITRAN96 data base (Rothman *et al.* 1998). Fig. 4 compares the experimental ro–vibrational spectrum of H_2O (Rothman *et al.* 1998) for these 819 transitions with the ab initio calculated spectra obtained by using the solution algorithms of PS (1997) and Searles and von Nagy-Felsobuki (1988, 1991, 1993). The root-mean-square (rms) between HITRAN 96 and our ab initio calculation for the line position and strength is 0.12 cm^{-1} and 3×10^{-22} cm molecule^{-1} respectively. The corresponding rms for the difference between PS (1997) and our results is 0.12 cm^{-1} and 8×10^{-23} cm molecule^{-1} respectively. It should be noted that PS 1997) empirically adjusted the PES to yield a maximum agreement with experiment for their solution algorithm.

Fig. 5 compares the ab initio ro–vibrational spectra of He_2O^{2+} and He_2S^{2+}, for all transitions up to the $\nu = 4$ and $J = 4$ level, using a threshold of 10^{-30} cm molecule^{-1} for the line strength. For He_2O^{2+} and He_2S^{2+} this resulted in 634 and 685 transitions respectively. These spectra are significantly different from water (as would be anticipated from consideration of the potential energy and dipole moment functions alone). Nevertheless, the differences in the nuclear spins also play an important role. For water, the nuclear spin statistic is either 1 or 3 depending on the symmetry of the state, whereas for the helide cations it is 0 or 1. It is hoped that the detailing of the ro–vibrational spectra for the low-lying transition will be of assistance for their detection in interstellar space.

6. Conclusions

Ab initio ro–vibrational eigenergies and line strengths were calculated using an Eckart-Watson Hamiltonian. The radiative transition probability integrals were determined using a novel adaptation of the HEG integration scheme. The solution algorithm yielded results for the $^1A_1$ ground state of H_2O, which are in excellent agreement with experiment (Rothman *et al.* 1998), and with the theoretical results of PS (1997). This solution algorithm has also been employed to calculate the ro–vibrational eigenergies and line strengths for the $^1A_1$ states of He_2O^{2+} and He_2S^{2+}, in order to facilitate their possible interstellar detection.

Acknowledgments

We wish to acknowledge the support of the ANU (Supercomputer Facility), the Australian Research Council and the Research Management Committee (University of Newcastle).

Mr Sudarko wishes to acknowledge support from AusAid for a University of Newcastle postgraduate scholarship and from the University of Jember for granting him leave to study abroad. We wish to thank Mr David Wilson for some helpful discussions.

References

Bernath, P., and Amano, T. (1982). *Phys. Rev. Lett.* **48**, 20.

Bieske, E. J., Soliva, A. M., Friedman, A., and Maier, J. P. (1992). *J. Chem. Phys.* **102**, 5570.

Carney, G. D., Langhoff, S. R., and Curtiss, L. A. (1977). *J. Chem. Phys.* **66**, 3724.

Dabrowski, L., and Herzberg, G. (1978). *J. Molec. Spectrosc.* **73**, 183.

Doherty, G., Hamilton, M. J., Burton, P. G., and von Nagy-Felsobuki, E. I. (1986). *Aust. J. Phys.* **39**, 749.

Dudley, W. W., and Williams, D. A. (1984). 'Interstellar Chemistry' (Academic: London).

E-PAPS (1997). AIP document E-JCPSA-106-4618; email: paps@aip.org. See Schwenke' s URL for more up-to-date information: http://george.arc.nasa.gov/~dschwenke/h2o/h2o.html.

Frenking, G., and Cremer, D. (1990). *In* 'Structure and Bonding', Vol. 73 (Ed. G. Frenking) (Springer: Heidelberg).

Frisch, M. J., *et al.* (1995). Gaussian 94, Revision D.3 (Gaussian Inc.: Pittsburgh).

Gabriel, W., Reinsch, E.-A., Rosmus, P., Carter, S., and Handy, N. C. (1993). *J. Chem. Phys.* **99**, 897.

Green, S. (1974). *Adv. Chem. Phys.* **25**, 179.

Green, S. (1981). *Annu. Rev. Phys. Chem.* **32**, 103.

Harris, D. O., Engerholm, G. G., and Gwinn, W. D. (1965). *J. Chem. Phys.* **43**, 1515.

Hughes, J. M., and von Nagy-Felsobuki, E. I. (1997). *J. Mol. Struct.* (*Theochem.*) **389**, 1.

Hughes, J. M., and von Nagy-Felsobuki, E. I. (1999). *J. Mol. Struct.* (*Theochem.*) **459**, 67.

Jørgensen, U. G. (1994). *In* 'Molecules in the Stellar Environment' (Ed. U. G. Jørgensen) (Springer: Berlin).

Koch, W., and Frenking, G. (1986). *J. Chem. Soc. Chem. Commun.* No. 1095.

Meuwly, M., Nizkorodov, S. A., Maier, J. P., and Bieske, E. J. (1996). *J. Chem. Phys.* **104**, 3876.

Meyer, W., Botschwina, P., and Burton, P. G. (1986). *J. Chem. Phys.* **84**, 891.

Munson, M. S. B., Franklin, J. L., and Field, F. H. (1963). *J. Phys. Chem.* **67**, 1542.

Oliphant, N., and Bartlett, R. J. (1994). *J. Chem. Phys.* **100**, 6550.

Partridge, H., and Schwenke, D. W. (1997). *J. Chem. Phys.* **106**, 4618.

Rothman, L. S., *et al.* (1992). *J. Quantitat. Spectrosc. Radiat. Transf.* **48**, 469.

Rothman, L. S., *et al.* (1998). *J. Quantitat. Spectrosc. Radiat. Transf.* **60**, 665.

Searles, D. J., and von Nagy-Felsobuki, E. I. (1988). *Am. J. Phys.* **56**, 444.

Searles, D. J., and von Nagy-Felsobuki, E. I. (1989). *Aust. J. Chem.* **42**, 737.

Searles, D. J., and von Nagy-Felsobuki, E. I. (1991*a*). *J. Chem. Phys.* **95**, 1107.

Searles, D. J., and von Nagy-Felsobuki, E. I. (1991*b*). *In* 'Vibrational Spectra and Structure', Vol. 19 (Ed. D. R. Durig) (Elsevier: New York).

Searles, D. J., and von Nagy-Felsobuki, E. I. (1992). *Comput. Phys. Commun.* **67**, 527.

Searles, D. J., and von Nagy-Felsobuki, E. I. (1993). 'Ab Initio Variational Calculations of Molecular Vibrational-Rotational Spectra' (Springer: Berlin).

Wang, F., and von Nagy-Felsobuki, E. I. (1992). *Aust. J. Phys.* **45**, 651.

Wang, F., and von Nagy-Felsobuki, E. I. (1995). *Spectrochimica Acta* A **51**, 1827.

Wong, M. W., Nobes, R. H., and Radom, L. (1987). *J. Chem. Soc. Chem. Commun.* No. 233.

Woon, D. E., and Dunning, T. H. (1994). *J. Chem. Phys.* **100**, 2975.

Woon, D. E., and Dunning, T. H. (1995). *J. Chem. Phys.* **103**, 4572.

Zare, R. N. (1987). 'Angular Momentum' (Wiley: New York).

Zobov, N. F., Polyansky, O. L., Tennyson, J., Lotoski, J. A., Colarusso, P., Zang, K.-Q., and Bernath, P. F. (1999). *J. Molec. Spectrosc.* **193**, 118.

Manuscript received 23 March, accepted 20 June 2000